JVST A
Journal of Vacuum Science & Technology A

ARTICLE

avs.scitation.org/journal/jva

Comparison of 2D crystals formed by dissociative adsorption of fluorinated and nonfluorinated alkyl iodides on Cu(111)

Cite as: J. Vac. Sci. Technol. A 39, 063211 (2021); doi: 10.1116/6.0001316
Submitted: 26 July 2021 · Accepted: 13 September 2021 ·
Published Online: 6 October 2021

Tedros A. Balema, Amanda M. Larson, Yicheng Wang, Dipna A. Patel, Krishna Kumar, and E. Charles H. Sykes[a)]

AFFILIATIONS

Department of Chemistry, Tufts University, Medford, Massachusetts 02155

Note: This paper is a part of the Special Collection Commemorating the Career of Pat Thiel.
[a)]**Author to whom correspondence should be addressed:** charles.sykes@tufts.edu

ABSTRACT

We report the comparison of a series of 2D molecular crystals formed from the intermediates of the dehalogenation reaction of iodoethane versus various fluorinated iodoalkanes on Cu(111). High-resolution scanning tunneling microscopy enables us to distinguish the alkyl groups from the iodine atoms, and we find that the ethyl groups and iodine atoms formed from the dissociation of ethyl iodide are well mixed. However, fluorination of the alkyl tail changes this behavior and leads to local segregation of the two species on the surface. We postulate that the low-polarizability and relatively large dipole moment of the fluorinated species drive the ordered assemblies of the fluorinated alkyl species on the surface and discuss this in the context of how solvophobicity can drive the clustering of fluorinated groups and, hence, phase separation.

I. INTRODUCTION

The design and construction of molecular arrays on surfaces are important for the development of many nanoscale systems for applications, such as molecular scale signal processing and energy modulation.[1–4] However, the relationships between the molecular structure and crystal packing cannot be predicted *a priori*. This is because many interactions are at play in the molecular self-assembly process including dispersion, dipole, quadrupole, hydrogen bonding, steric, and through-surface interactions. In order to study noncovalent interactions that result from saturated fluorocarbons, we focus on a series of alkyl halides that contain either a terminal methyl or a trifluoromethyl group on Cu(111). The surface chemistry of alkyl halides on copper is also of great significance in various chemical processes such as the Ullmann coupling reaction,[5] the Muller–Rochow method for organochlorosilane production,[6,7] and β-hydride elimination in alkyl species to yield their corresponding olefin.[8,9] These chemistries are possible due to the reaction selectivity of copper catalysts that facilitate carbon−carbon coupling and the copper catalyst's effectiveness in the breaking of most carbon−halide bonds.[10,11]

Replacement of methyl ($-CH_3$) with trifluoromethyl ($-CF_3$) groups results in fewer dispersion interactions with surrounding molecules due to the extremely low polarizibility of fluorine atoms.[12,13] This phenomenon can manifest itself in "solvophobicity" where clustering of trifluoromethyl groups drives phase separation.[14,15] At a particular size and number, such segregation becomes entropically unviable and leads to "islands" of intervening groups depending on the molecular environment.[15,16] Although the $-CH_3$ group has roughly half the molar volume of a $-CF_3$ group, it can be statistically replaced by the latter in crystals (solid solutions).[13,17] These observations would predict that some local phase separation would occur where a large, polarizable iodine atom would segregate from $-CF_3$ groups that drive the structures highlighted later in this article. Such effects have been seen in peptide and protein assemblies[18,19] and also in the context of the nonpolar environment of membranes.[20]

Herein, we report the comparison of a series of 2D molecular crystals formed from the intermediates of the dehalogenation reaction of iodoethane versus various fluorinated iodoalkanes on Cu(111). The fluorinated molecules in this study are 1,1,1-trifluoro-2-iodoethane,

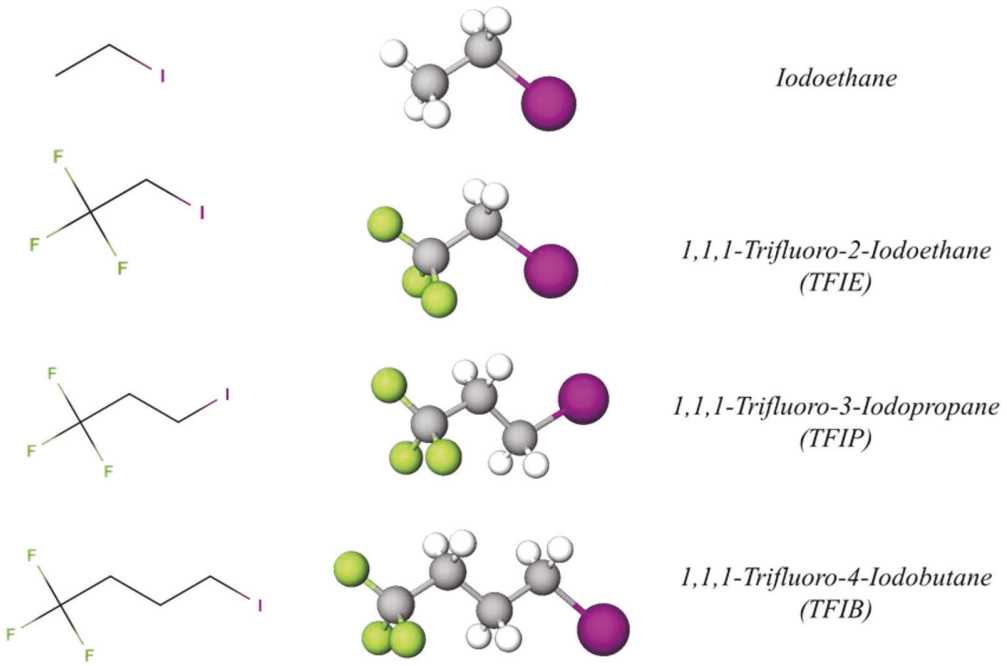

FIG. 1. Schematic of the molecules and their molecular structures that are presented in this study. The abbreviations TFIE, TFIP, and TFIB will be used throughout the text.

1,1,1-trifluoro-3-iodopropane, and 1,1,1-trifluoro-4-iodobutane. For the sake of brevity, they are labelled as TFIE, TFIP, and TFIB, respectively, as shown below in Fig. 1.

The reaction intermediates that this study focuses on are outlined by the blue rectangle, as shown in the reaction scheme in Fig. 2. Using scanning tunneling microscopy (STM), we were able to image the atomic-scale structural differences in the resulting 2D crystal formations. We show that simply changing the alkyl chain of a given haloalkane can yield significantly different structures. Such findings can contribute to understanding the relationship between polarity alongside conformational entropy in 2D crystal formation, hence elucidating an aspect of 2D engineering.

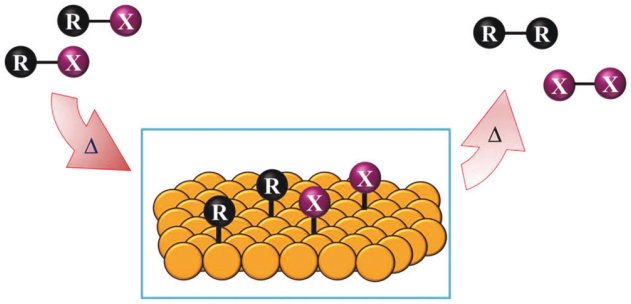

FIG. 2. Schematic of the dehalogenation reaction of the iodoalkanes on Cu(111) in this study. The intermediates of interest are outlined in the blue rectangle. R represents the alkyl/fluoroalkyl group and X represents iodine.

II. METHODS

The low-temperature-STM was operated with a base pressure of $<1 \times 10^{-11}$ mbar. Iodoethane was acquired from Sigma Aldrich at 99% purity. 1,1,1-Trifluoro-2-iodoethane (99% purity), 1,1,1-Trifluoro-3-iodopropane (98% purity), and 1,1,1-trifluoro-4-iodobutane (98% purity) were acquired from Alfa Aesar. The chemicals were further degassed by multiple freeze/pump/thaw cycles. Each chemical was vapor deposited on to a Cu(111) sample held at 5 K through a collimated molecular doser attached to a precision leak valve. Samples were annealed from 5 K up to 160 K by removing the sample from the cryogenically cooled stage of the STM and placing it into a sample holder held at room temperature in the UHV chamber in order to break the C-I bond and equilibrate the reaction intermediates.[21,22] The crystal was then cooled back to 5 K by putting it back into the STM stage for imaging. While alkyl groups typically undergo hydrogen elimination and desorb as alkenes just above room temperature on Cu(111), the iodine atoms are very stable and desorption does not occur until temperatures around 900 K are reached.[21]

III. RESULTS AND DISCUSSION

We begin by comparing the structure of dissociated fluorinated and nonfluorinated ethyl iodide. As can be seen in Fig. 3(a), both species assemble into large 2D islands surrounded by areas of

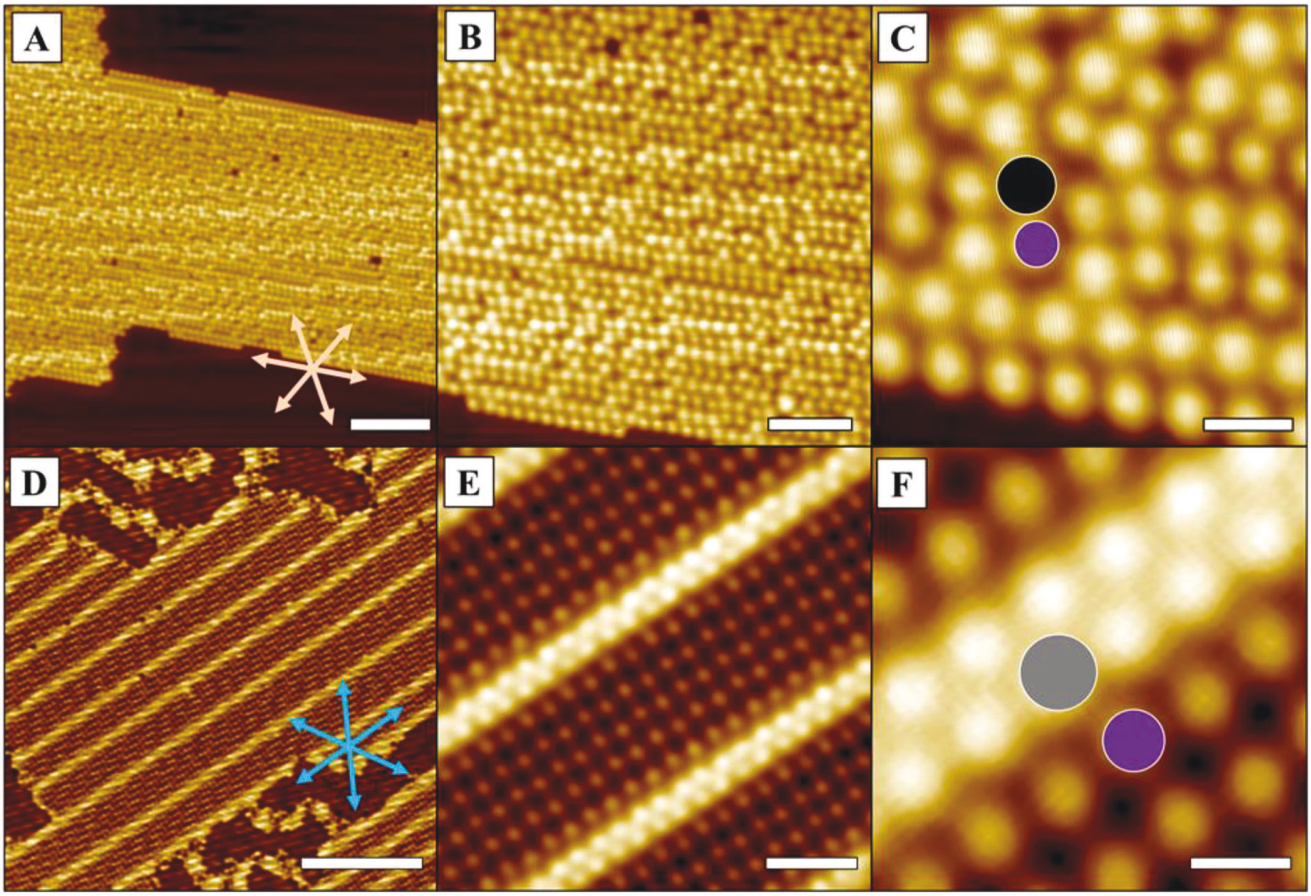

FIG. 3. 5 K STM images of (a) large domain of dissociated iodoethane on Cu(111). The close-pack directions of the underlying Cu(111) surface are indicated with orange arrows. (b) and (c) High-resolution images of the large domain in (a) with the ethyl moiety highlighted in black and an iodine atom highlighted in purple. (d) Large domain of dissociated 1,1,1-trifluoro-2-iodoethane (TFIE) on Cu(111). The $\sqrt{3}$ directions of the underlying Cu(111) surface are indicated with blue arrows. (e) and (f) High-resolution images of the large domain of the TFIE in which the trifluoro-ethyl moiety is highlighted in gray and iodine highlighted in purple. Scanning conditions: (a) +120 mV, 90 pA, scale bar: 5 nm; (b) +120 mV, 90 pA, scale bar: 2.5 nm; (c) +120 mV, 90 pA, scale bar: 0.5 nm; (d) +70 mV, 560 pA, scale bar: 10 nm; (e) +70 mV, 560 pA, scale bar: 4 nm; and (f) +70 mV, 600 pA, scale bar: 0.5 nm.

bare Cu. In both cases, the islands are composed of ethyl/fluorinated ethyl groups mixed with iodine atoms. However, from the high-resolution STM images of these islands, it is clear that the fluorinated ethyl groups arrange very differently from the non-fluorinated ethyl groups and that the large mixed islands are oriented differently to the underlying Cu(111) lattice. As we will demonstrate later in the article, the smaller protrusions in these images correspond to iodine atoms and the larger, brighter protrusions to the ethyl/fluoroethyl species. STM images like those shown in Figs. 3(b) and 3(e) reveal that while the ethyl groups arrange semirandomly in the sea of iodine atoms, the fluorinated ethyl groups form highly ordered structures consisting of 1D stripes of the fluorinated ethyl groups that are surrounded by iodine atoms.

Upon closer inspection of the molecular arrays formed by the dissociative adsorption of TFIE, as shown in Fig. 4(a), it can be seen that the components are segregated and have distinct adsorption structures. The fluorinated ethyl groups form two-moleculewide 1D chains in which the fluorinated ethyl groups are locally packed in a $(\sqrt{3}\times\sqrt{3})$ unit cell. Meanwhile, the iodine atoms are packed in a pseudosquare unit cell dimensions with dimensions $\left(2\sqrt{3}\times\sqrt{\frac{121}{48}}\right)$. Interestingly, to the best of our knowledge, iodine atoms always arrange hexagonally, typically $(\sqrt{3}\times\sqrt{3})R$ 30°, on (111) metal surfaces, as seen in Fig. 5(a) for iodine atoms on Cu(111).[23,24] The pseudosquare packing behavior observed in the mixed fluorinated ethyl/iodine atom islands is reminiscent of the square packing of iodine on (100) metal surfaces; however, we observe no evidence (etch pits, monolayer high islands) for reconstruction of Cu(111).[25–29]

Before moving to a discussion of longer chain fluorinated alkanes, we present data that support our assignments of the

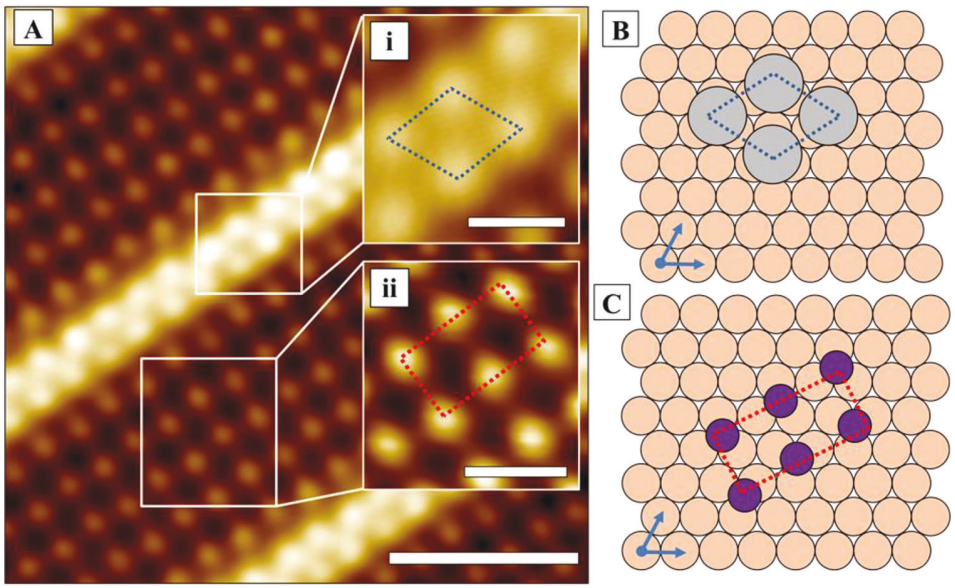

FIG. 4. (a) 5 K STM image of dissociatively adsorbed TFIE on Cu(111). Inset: (i) High-resolution image of the fluorinated ethyl groups with the unit cell is highlighted with dark blue dotted lines. (ii) High-resolution image of the iodine atoms with the unit cell is highlighted with red dotted lines. (b) Model schematic of the $(\sqrt{3} \times \sqrt{3})$ unit cell formed by the fluorinated ethyl groups as highlighted with blue dotted lines. (c) Model schematic of the $\left(2\sqrt{3} \times \sqrt{\frac{121}{48}}\right)$ unit cell formed by the iodine atoms as highlighted with red dotted lines. Scanning conditions: +70 mV, 540 pA, scale bar: 1.5 nm. Inset scale bars: 0.5 nm.

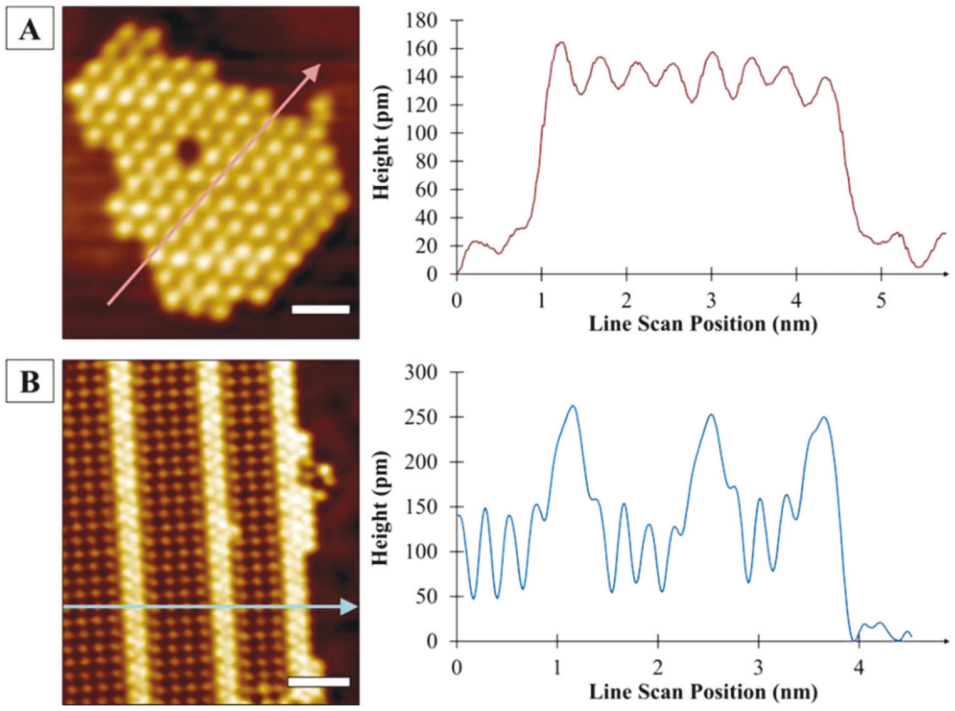

FIG. 5. STM images with their accompanying topographic line scan as shown by colored arrows: (a) a domain of pure iodine atoms on Cu(111); (b) 2D island of dissociated 1,1,1-trifluoro-2-iodoethane on Cu(111). Imaging conditions: (a) +120 mV, 240 pA; (b) +50 mV, 80 pA. Scale bars: 1 nm.

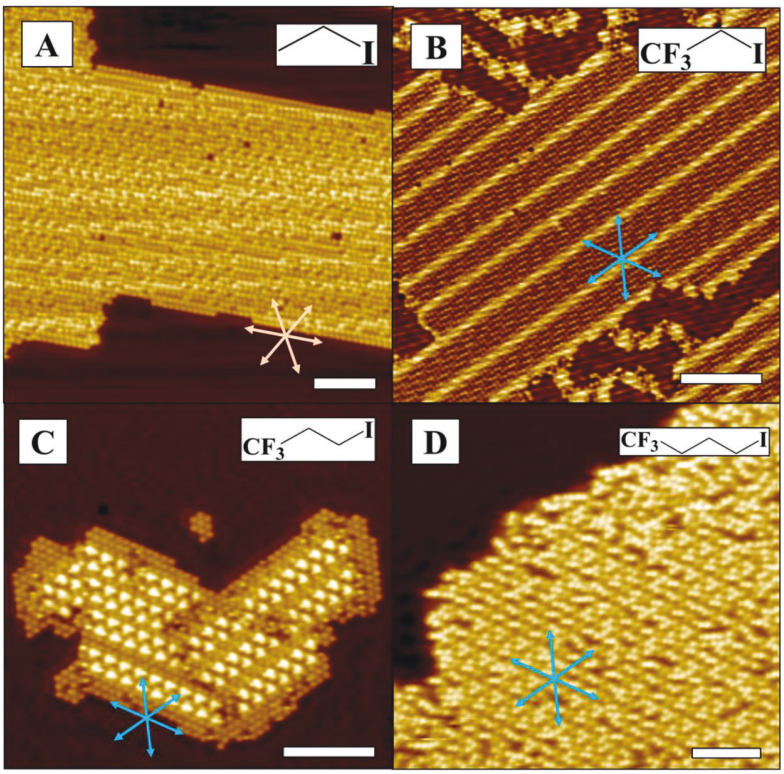

FIG. 6. STM images of large domains on Cu(111) of (a) iodoethane. The close-packed directions are indicated with orange arrows; (b) TFIE, (c) TFIP, and (d) TFIB. The $\sqrt{3}$ directions are indicated with blue arrows. Imaging conditions: (a) +120 mV, 90 pA, scale bar: 4 nm; (b) +70 mV, 560 pA, scale bar: 4 nm; (c) −170 mV, 270 pA, scale bar: 5 nm; and (d) +70 mV, 200 pA, scale bar: 5 nm.

identity of the iodine atoms and fluorinated ethyl groups as previously mentioned. Specifically, topographic STM line scans of the 2D islands formed by the dissociative adsorption of the alkyl halides were performed. The apparent height of features in these line scans was then compared to the height of domains of pure iodine atoms on Cu(111). A representative set of these measurements is shown in Fig. 5, and the apparent height of iodine atoms (panel A) is ∼120 pm. Panel B shows the iodine/fluoroethyl mix in which the features consistent with iodine atoms are ∼120 pm high versus the fluoroethyl groups that are ∼250 pm in height.

To determine whether the length of the alkyl chain has a significant contribution to the formation of 2D domains, iodoethane and TFIE were compared with TFIP and TFIB, as shown in Fig. 6. The difference in structure is very apparent as the alkyl chain is increased from 2 to 3 and 4 carbons. In Fig. 6(c), it is observed that the fluorinated propyl species, which again appear brighter than the surrounding iodine atoms, are present in small triangular groupings, separated by iodine atoms. Meanwhile, in Fig. 6(d), the structure formed from fluorinated butyl species and iodine atoms appears to be more disordered, but with regions of short-range order in which the fluorinated butyl species again appear in small triangular clusters surrounded by iodine atoms.

On closer inspection of the domains formed by dissociated TFIP, just like in the case of the TFIE, the fluorinated moieties orient themselves in the $\sqrt{3}$ orientation of the underlying Cu(111) surface with the molecules arranged in two rows with its unit cell dimensions being $(2\sqrt{3} \times 2\sqrt{3})$ as seen in Figs. 7(a) and 7(b). These domains are not as large compared to TFIE, instead what was observed was that the TFIP moieties are surrounded by iodine atoms. Between the TFIP row pairs, there was always at least a row of iodine atoms; however, the iodine rows were nowhere near as expansive in size or degree of order compared to the TFIE domains. Meanwhile, in TFIB, the domains are somewhat less ordered. It is observed that there are limited regions of short-range order within the large domains as shown in Fig. 7(c). Zooming into these limited regions in the inset of Fig. 7(c), even though there is a semblance of overall order oriented in a $\sqrt{3}$ direction, a unit cell cannot be determined.

Overall, we find that the ethyl groups and iodine atoms formed from the dissociation of ethyl iodide are well mixed. However, fluorination of the alkyl tail changes this behavior and leads to local segregation of the two species on the surface. We postulate that the relatively large dipole moment of the fluorinated species (e.g., the TFIE moiety has an associated dipole of ∼2.3 D)[30] drives the ordered assemblies of the alkyl species on the surface. For TFIE, the trifluoroethyl species align in highly ordered 1D rows that are two molecules wide. This is consistent with a picture in which the molecules orient their dipoles to align in a zig-zag-like pattern,[31–35] as seen in Fig. 8.

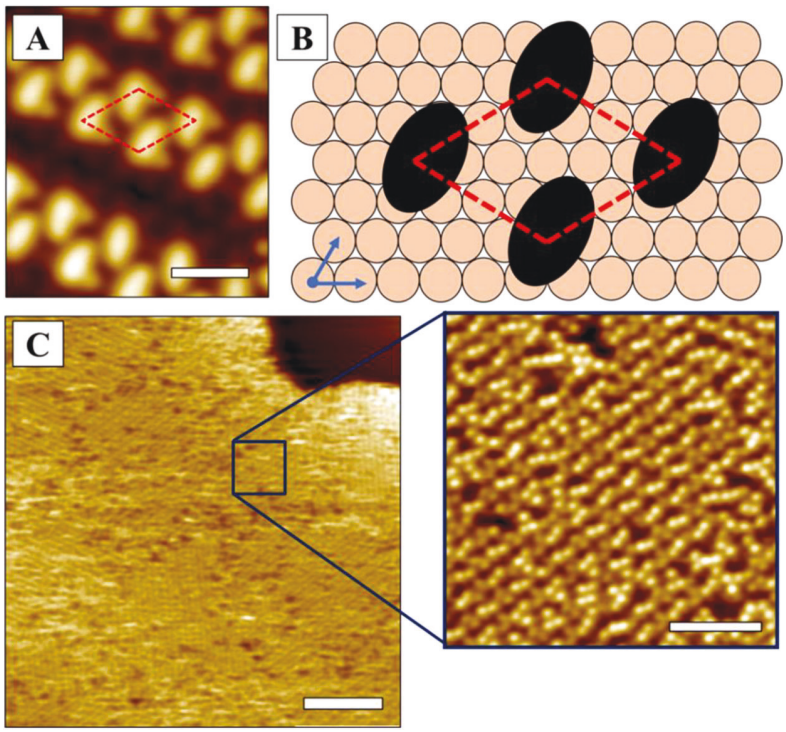

FIG. 7. (a) 5 K STM image of TFIP on Cu(111). The TFIP unit cell is highlighted with red dotted lines; (b) model schematic of the TFIP moiety unit cell, and its dimensions are ($2\sqrt{3} \times 2\sqrt{3}$). The unit cell is highlighted with red dotted lines; (c) 5 K STM image of a large domain of TFIB on Cu(111). Inset: close-up of a more-ordered region. Imaging conditions: (a) −300 mV, 40 pA, scale bar: 1 nm; (c) +70 mV, 200 pA, scale bar: 15 nm, inset scale bar: 4 nm.

Furthermore, when molecules adsorb on a surface, there is charge transfer between the molecule and the surface, leading in most cases to a dipole moment perpendicular to the surface. In some cases, the dipole-dipole repulsion of these surface-induced dipoles leads to molecular assemblies limited to just a few molecules or the formation of magic clusters.[36–38] In the present case, we postulate that this charge transfer effect limits the interaction of the trifluoroethyl species to 1D rows and for the C3 and C4 fluorinated alkyl species, to small groups of three molecules, separated by iodine atoms in order to prevent dipole-dipole repulsion between adjacent molecules in large grouping destabilizing the whole assembly. This behavior is in stark contrast to the nonfluorinated ethyl iodide case in which the two species are well mixed at all length scales. When discussing the ordering behavior observed in these systems, it is informative to do so in the context of dispersion and interactions of a trifluoromethyl group that is entirely different from that of a methyl terminus.[39–41] The present case is particularly interesting in this respect because of the very different polarizabilities of iodine/ethyl versus trifluoroalkyl species. In this study, the alkyl groups studied contain either two halves that are both reasonably polarizable or a terminal trifluoromethyl group that has diminished capacity to participate in van der Waals interactions. Take TFIP, for example, it has a lower half (CH_2CH_2) that is polarizable and can participate in van der Waals interactions and a top part (CF_3) that is dipolar but nonpolarizable. This results in local segregation driven by annealing kinetics, and the size of the phase-separated domains is determined by entropy and packing considerations.[15,16] We have previously observed such segregated domains in larger lipid-lipid phase separation.[15] Such control over the size and orientation of functional groups on catalytic metals like Cu may be useful in engineering surfaces with specific architectures and catalytic functionalities.

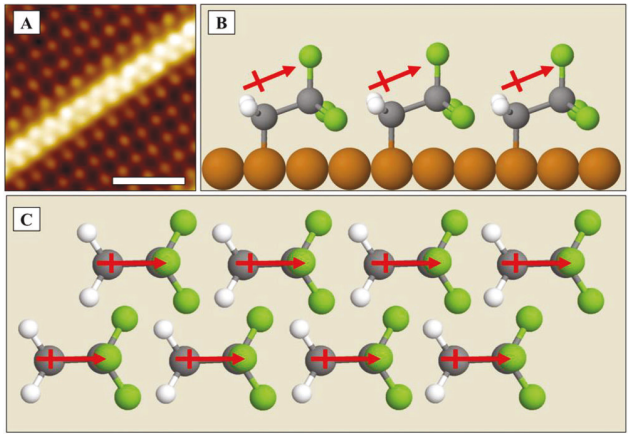

FIG. 8. (a) STM image of dissociated TFIE on Cu(111). Schematics of trifluoroethyl alignment on Cu(111) with their dipole direction indicated in red: (b) Side view. (c) Top view. Imaging conditions: (a) 70 mV, 560 pA, scale bar: 2 nm.

IV. CONCLUSIONS

Our data demonstrate the distinct differences between the self-assembly of fluorinated and nonfluorinated alkyl groups formed from the dissociative adsorption of a range of modified alkyl iodides on Cu(111). While ethyl groups and iodine atoms are well mixed, the dissociation of fluorinated alkyl halides leads to the formation of linear structures in the case of trifluoroethyl groups that are well separated from one another by iodine atoms and small clusters for the trifluoropropyl and butyl species. This provides molecular-scale resolution of the origins of segregation of fluorinated species using a well-defined single crystal system that may be amenable to modelling and provides a method by which the self-assembly of linear or locally clustered surface architectures can be performed.

ACKNOWLEDGMENTS

The authors thank the U.S. National Science Foundation (Grant No. CBET-2034911) for support of the project.

DATA AVAILABILITY

The data that support the findings of this study are available from the corresponding author upon reasonable request.

REFERENCES

[1]J. A. Lloyd *et al.*, Nano Lett. **16**, 1884 (2016).
[2]L. I. Clarke, D. Horinek, G. S. Kottas, T. F. Magnera, T. P. Hinderer, J. Michl, and J. C. Price, Nanotechnology **13**, 533 (2002).
[3]G. S. Kottas, L. I. Clarke, D. Horinek, and J. Michl, Chem. Rev. **105**, 1281 (2005).
[4]N. A. Wasio, D. P. Slough, Z. C. Smith, C. J. Ivimey, S. W. Thomas III, Y.-S. Lin, and E. C. H. Sykes, Nat. Commun. **8**, 16057 (2017).
[5]F. Ullmann and Jean Bielecki, Chemische Berichte **34**(2), 2174 (1901).
[6]E. G. Rochow and W. F. Gilliam, J. Am. Chem. Soc. **67**, 1772 (1945).
[7]D.-H. Sun, B. E. Bent, A. P. Wright, and B. M. Naasz, J. Mol. Catal. A Chem. **131**, 169 (1998).
[8]J. G. Forbes and A. J. Gellman, J. Am. Chem. Soc. **115**, 6277 (1993).
[9]C. J. Jenks, M. Xi, M. X. Yang, and B. E. Bent, J. Phys. Chem. **98**, 2152 (1994).
[10]J. L. Lin and B. E. Bent, J. Phys. Chem. **96**, 8529 (1992).
[11]C. Chao-Ming and B. E. Bent, Surf. Sci. **279**, 79 (1992).
[12]D. Seebach, Angew. Chem. Int. Ed. Engl. **29**, 1320 (1990).
[13]D. Seebach, P. Renaud, W. B. Schweizer, M. F. Züger, and M.-J. Brienne, Helv. Chim. Acta **67**, 1843 (1984).
[14]K. E. Myers and K. Kumar, J. Am. Chem. Soc. **122**, 12025 (2000).
[15]N. C. Yoder, V. Kalsani, S. Schuy, R. Vogel, A. Janshoff, and K. Kumar, J. Am. Chem. Soc. **129**, 9037 (2007).
[16]S. Schuy, S. Faiss, N. C. Yoder, V. Kalsani, K. Kumar, A. Janshoff, and R. Vogel, J. Phys. Chem. B **112**, 8250 (2008).
[17]D. O'Hagan and H. S. Rzepa, Chem. Commun. 645 (1997).
[18]B. Bilgiçer, X. Xing, and K. Kumar, J. Am. Chem. Soc. **123**, 11815 (2001).
[19]B. Bilgiçer, A. Fichera, and K. Kumar, J. Am. Chem. Soc. **123**, 4393 (2001).
[20]B. Bilgicer and K. Kumar, Proc. Natl. Acad. Sci. U.S.A. **101**, 15324 (2004).
[21]C. J. Jenks, B. E. Bent, N. Bernstein, and F. Zaera, J. Phys. Chem. B **104**, 3008 (2000).
[22]D. Sung and A. J. Gellman, Surf. Sci. **551**, 59 (2004).
[23]J. Inukai, Y. Osawa, and K. Itaya, J. Phys. Chem. B **102**, 10034 (1998).
[24]I. T. McCrum, S. A. Akhade, and M. J. Janik, Electrochim. Acta **173**, 302 (2015).
[25]T. E. Felter and A. T. Hubbard, J. Electroanal. Chem. Interf. Electrochem. **100**, 473 (1979).
[26]B. V. Andryushechkin, K. N. Eltsov, V. M. Shevlyuga, U. Bardi, and B. Cortigiani, Surf. Sci. **497**, 59 (2002).
[27]B. V. Andryushechkin, G. M. Zhidomirov, K. N. Eltsov, Y. V. Hladchanka, and A. A. Korlyukov, Phys. Rev. B **80**, 125409 (2009).
[28]P. H. Citrin, P. Eisenberger, and R. C. Hewitt, Phys. Rev. Lett. **45**, 1948 (1980).
[29]N. A. Kautz and S. A. Kandel, J. Phys. Chem. C **113**, 19286 (2009).
[30]D. R. Lide, *CRC Handbook of Chemistry and Physics: A Ready-Reference Book of Chemical and Physical Data*, 74th ed. (CRC, Boca Raton, FL, 1995).
[31]D. A. Kunkel *et al.*, J. Chem. Phys. **142**, 101921 (2015).
[32]I. Custovic, D. Teyssieux, J. Jeannoutot, S. Lamare, F. Palmino, H. Abbasian, A. Rochefort, and F. Chérioux, Nanoscale **12**, 17399 (2020).
[33]W. Tong, Y. Xue, and M. B. Zimmt, J. Phys. Chem. C **114**, 20783 (2010).
[34]M. Dong, K. Miao, Y. Hu, J. Wu, J. Li, P. Pang, X. Miao, and W. Deng, Phys. Chem. Chem. Phys. **19**, 31113 (2017).
[35]M. K. Kim, Y. Xue, T. Pašková, and M. B. Zimmt, Phys. Chem. Chem. Phys. **15**, 12466 (2013).
[36]A. D. Jewell, S. M. Simpson, A. Enders, E. Zurek, and E. C. H. Sykes, J. Phys. Chem. Lett. **3**, 2069 (2012).
[37]C. J. Murphy *et al.*, J. Phys. Chem. C **120**, 6020 (2016).
[38]A. Enders, N. Malinowski, D. Ievlev, E. Zurek, J. Autschbach, and K. Kern, J. Chem. Phys. **125**, 191102 (2006).
[39]E. R. Johnson, I. D. Mackie, and G. A. DiLabio, J. Phys. Org. Chem. **22**, 1127 (2009).
[40]M. S. Christian, A. Otero-de-la-Roza, and E. R. Johnson, J. Chem. Theory Comput. **12**, 3305 (2016).
[41]A. Kumar and W. J. Meath, Mol. Phys. **54**, 823 (1985).